

## APPENDIX A: Levenberg Marquadt Fitting Algorithm

---



---

Levenberg-Marquadt (L-M) fitting algorithm is popularly used in the least squares fitting problem.

Consider data points  $(x_i, y_i)$  of a set of  $N$  measured data. the most likely estimate of the model parameters  $a = \{a_1, a_2, \dots, a_M\}$  is obtained by minimizing the quantity  $\chi^2$  :

$$\chi^2(a) = \sum_{i=1}^N (y_i - f(x_i - a))^2$$

(1)

Just like any other numeric minimization algorithm, the L-M algorithm is an iterative procedure. To start a minimization, the initial get for the user provides the initial guess for the parameters vector  $a = \{a_1, a_2, \dots, a_M\}$

At each iteration step, the parameter vector  $a$  is replaced by a new estimate  $a + \delta$ . To determine  $\delta$ , the function  $f(x, a + \delta)$  is approximated linearly.

$$f(x, a + \delta) \approx f(x, a) + \underline{\underline{J}} \cdot \delta \tag{2}$$

The matrix  $\underline{\underline{J}}$  is a Jacobian matrix containing partial derivative of the function  $f$  in accordance with the parameter  $a_j$  :

$$J_{ij} = \frac{\partial f(x_i, a)}{\partial a_j} \tag{3}$$

Substituting (2) in (1), we get

$$\chi^2(a + \delta) = \sum_{i=1}^N (y_i - f(x_i - a) - \underline{\underline{J}} \cdot \delta)^2 \tag{4}$$

The same can be re-written in vector notation as

$$\chi^2(a + \delta) \approx \left\| y - f(a) - \underline{\underline{J}} \cdot \delta \right\|^2 \tag{5}$$

Differentiating *wrt*  $\delta$  and equating the result to zero, we get

$$(\underline{\underline{J}}^T \underline{\underline{J}}) \cdot \delta = \underline{\underline{J}}^T \cdot (y - f(a)) \quad (6)$$

This is the Gauss-Newton algorithm to solve a set of linear equations for  $\delta$ . Levenberg replaced this equation by

$$(\underline{\underline{J}}^T \underline{\underline{J}} - \lambda \cdot \tau) \cdot \delta = \underline{\underline{J}}^T \cdot (y - f(a)) \quad (7)$$

where  $\tau$  is the identity matrix. The non-negative damping factor  $\lambda$  is adjusted at each iteration. If the decrease in  $\chi^2$  is rapid, a smaller value of  $\lambda$  can be used and the algorithm is similar to the Gauss-Newton algorithm. If the iteration is low,  $\lambda$  can be increased and the step will be taken approximately in the direction of the gradient.

Marquadt improved the algorithm by scaling each component of the gradient according to the curvature, so that there is larger movement along the directions where the gradient is smaller, thus avoiding slow convergence in the direction of the small gradient. To facilitate this, Marquadt replaced the identity matrix  $\tau$  with a diagonal matrix consisting of diagonal elements of  $(\underline{\underline{J}}^T \underline{\underline{J}})$ , resulting in the L-M algorithm:

$$(\underline{\underline{J}}^T \underline{\underline{J}} - \lambda \cdot (\underline{\underline{J}}^T \underline{\underline{J}})) \cdot \delta = \underline{\underline{J}}^T \cdot (y - f(a)) \quad (8)$$

The choice of damping factor  $\lambda$  is not obvious. Marquadt recommended starting with a value  $\lambda = \lambda_0$  and a factor  $\nu > 1$ . Depending on the value of  $\chi^2$ , the damping factor will be replaced after each step by  $\lambda/\nu$  or  $\lambda \cdot \nu$ .

An important point about the L-M algorithm is that it finds only a *local* minimum like all other iterative procedures, not a global minimum.

## APPENDIX B: Data and fits

### 1. Chapter 6: Pt/Ni/C Multilayer system

#### (i) Low angle

#### a) Pristine Sample

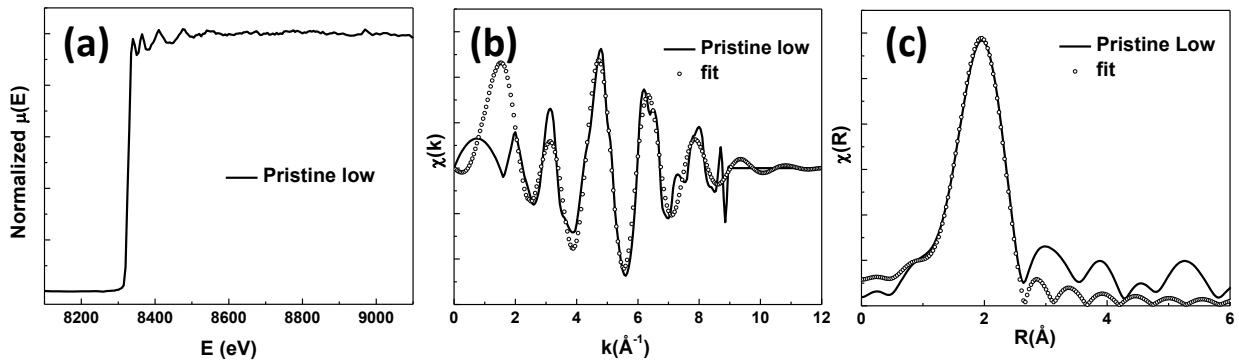


Fig. 1: (a) Ni K edge XAFS data in E space for pristine sample at low angle. Comparison of data with fit in (b) k-space and (c) r-space.

#### b) Irradiated Sample

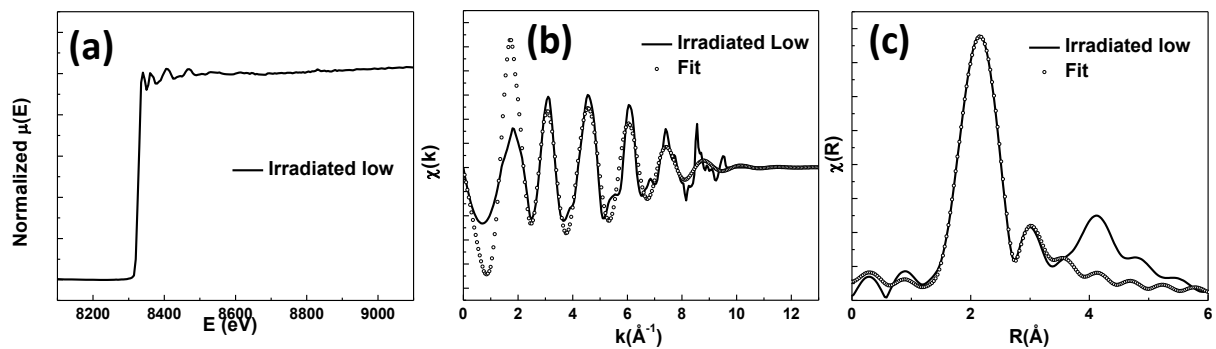


Fig. 2: (a) Ni K edge XAFS data in E space for irradiated sample at low angle. Comparison of data with fit in (b) k-space and (c) r-space.

(j) High angle

a) Pristine Sample

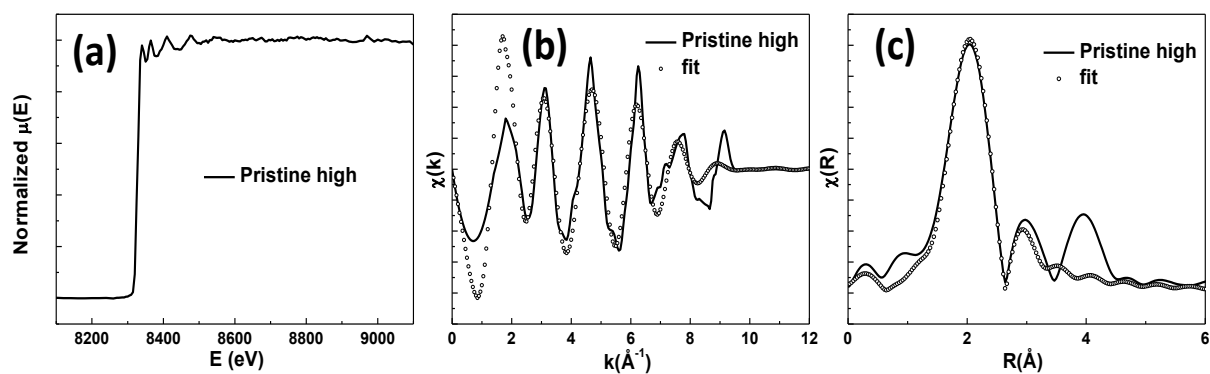


Fig. 3: (a) Ni K edge XAFS data in E space for pristine sample at high angle. Comparison of data with fit in (b) k-space and (c) r-space.

b) Irradiated Sample

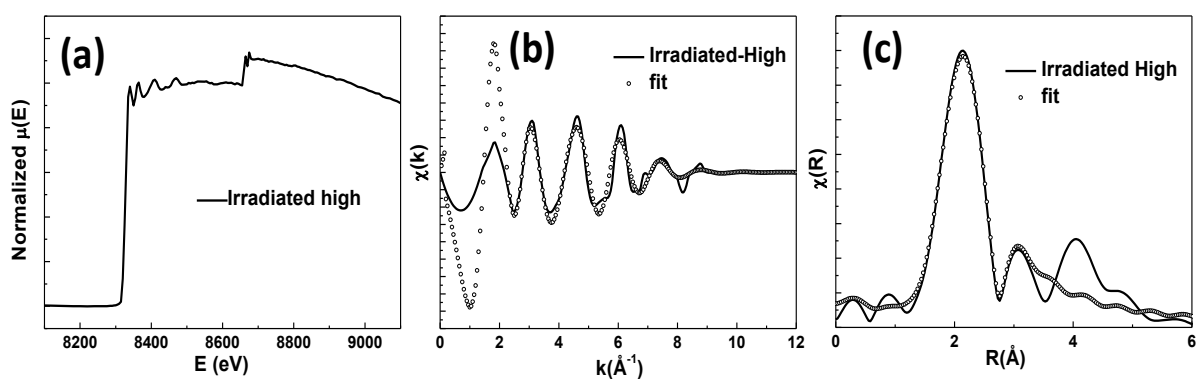


Fig. 4: (a) Ni K edge XAFS data in E space for irradiated sample at high angle. Comparison of data with fit in (b) k-space and (c) r-space.

## 2. Chapter 7: Ag/Pt nanorods in silica matrix

### a) Pristine sample

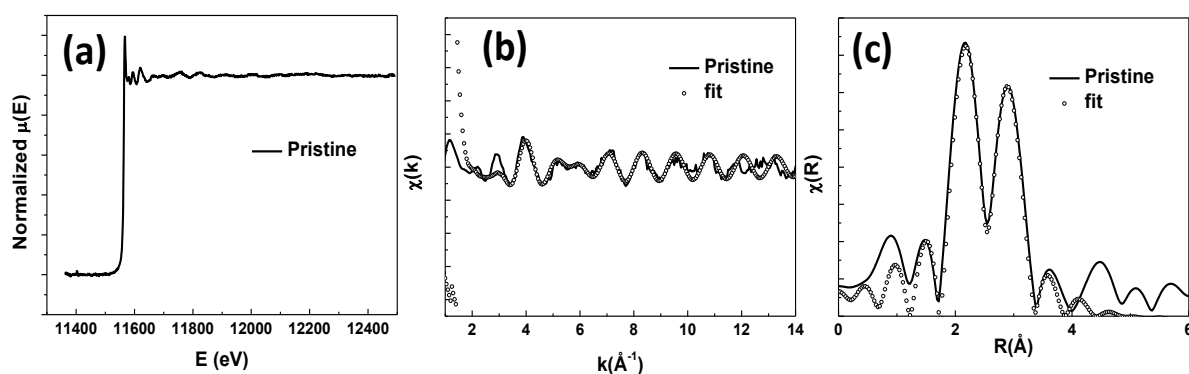


Fig. 5: (a) Pt L3 edge XAFS data in E space for pristine sample. Comparison of data with fit in (b) k-space and (c) r-space.

### b) SHI Irradiated samples

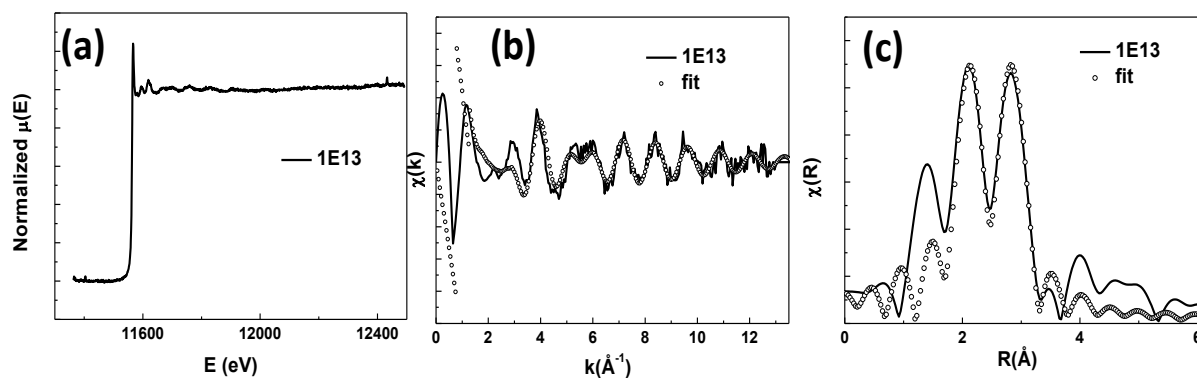


Fig. 6: (a) Pt L3 edge XAFS data in E space for sample irradiated at  $1 \times 10^{13}$  ions/cm<sup>2</sup>. Comparison of data with fit in (b) k-space and (c) r-space.

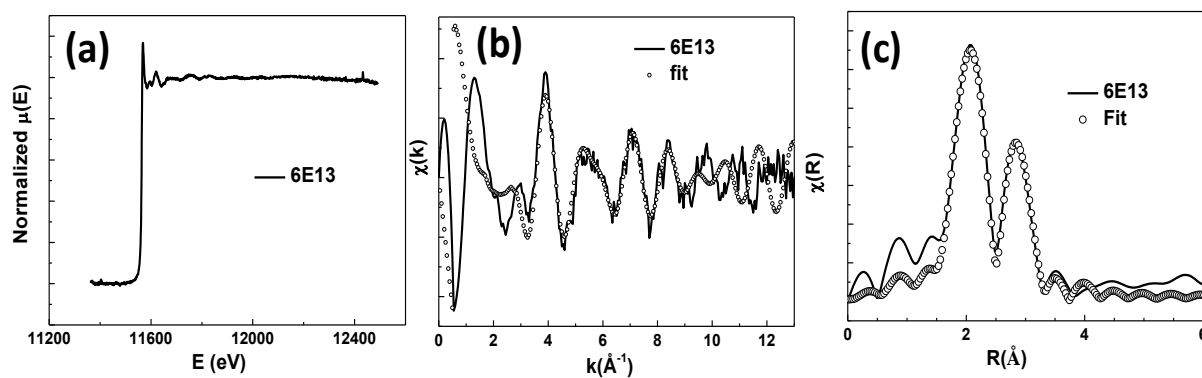


Fig. 7: (a) Pt L3 edge XAFS data in E space for sample irradiated at  $6 \times 10^{13}$  ions/cm<sup>2</sup>. Comparison of data with fit in (b) k-space and (c) r-space.

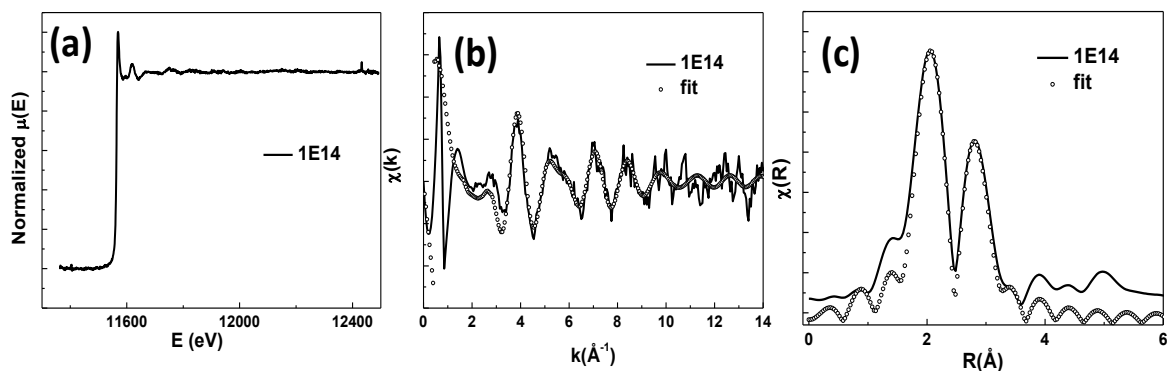


Fig. 8: (a) Pt L3 edge XAFS data in E space for sample irradiated at  $1 \times 10^{14}$  ions/cm<sup>2</sup>. Comparison of data with fit in (b) k-space and (c) r-space

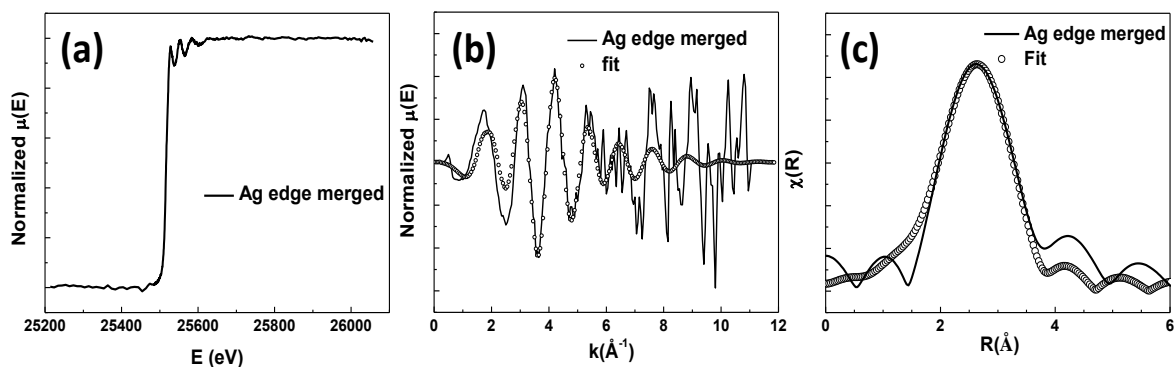


Fig. 9: (a) Ag K edge XAFS data in E space for merged data set of all samples. Comparison of data with fit in (b) k-space and (c) r-space

### 3. Chapter 8: Ayurvedic nanodrug

#### a) Rasasindura

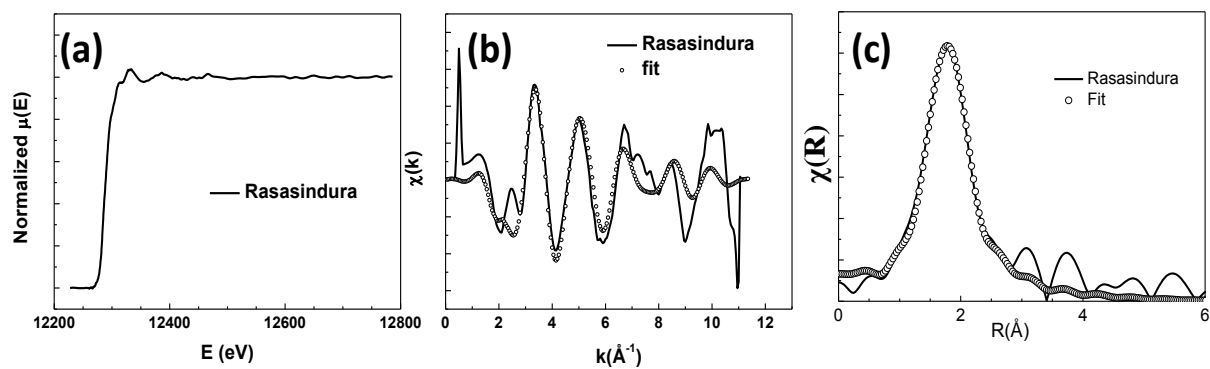


Fig. 10: (a) Hg L3 edge XAFS data in E space for Rasasindura. Comparison of data with fit in (b) k-space and (c) r-space.

b) Red HgS (lab)

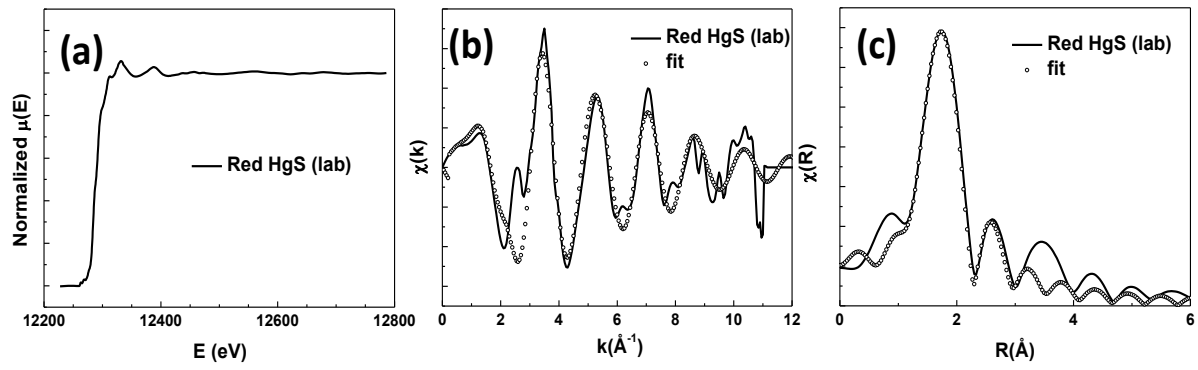


Fig. 11: (a) Hg L3 edge XAFS data in E space for Red HgS (lab). Comparison of data with fit in (b) k-space and (c) r-space.